

# A High-Capacity Interleaved Parallel Full-Bridge LLC Converter for External Charging Applications

Kada Sudheer<sup>1</sup>, K Rajasekhar<sup>2</sup>

<sup>1</sup>Department of Electronics and Communication Engineering, UCEK, JNTUK, Kakinada, India

<sup>2</sup>Assistant Professor, Department of Electronics and Communication Engineering, UCEK, JNTUK, Kakinada, India

**Abstract:**-This paper explores innovative converter designs tailored to meet the evolving demands of modern electric vehicle (EV) charging and power conversion systems. The first investigation centres on an AC to DC converter featuring an input series inductor and an output capacitor, enhancing power factor correction, reducing harmonics, and optimizing voltage regulation through advanced simulation tools. Comparative analysis highlights its superior power factor maintenance and efficiency. The second proposal introduces an interleaved parallel LLC (Inductor-Inductor-Capacitor) DC/DC converter, incorporating hybrid pulse frequency modulation (PFM) and pulse width modulation (PWM) control. This design extends the adjustable output voltage range, ensuring precise voltage control. A meticulous analysis and parametric design demonstrate an output voltage range of 50–80 V and a maximum power of 20 kW through simulation results. These innovations hold promise for various applications, including renewable energy, electronic device power supplies, and EV charging, offering practical solutions to enhance energy efficiency and power quality across modern electrical systems and EV infrastructure.

**Keywords:** AC to DC converter, DC/DC converter, series inductor, output capacitor, power factor correction(PFC), efficiency, renewable energy, electric vehicle charger, PFM, PWM, Off-Board Charger(OBC), Resonance Frequency.

## 1. Introduction

The transformation of alternating current (AC) into direct current (DC) is a fundamental procedure with significant ramifications in the ever-evolving field of modern electronics [1]. This fundamental change serves as the foundation for many electrical systems and gadgets, from consumer electronics to heavy equipment. Concurrently, the automotive industry is undergoing a paradigm shift by championing electric vehicles (EVs) in response to environmental and health concerns associated with traditional fossil fuel-powered vehicles. This transition necessitates the development of a robust and sustainable EV charging infrastructure.

In the realm of AC to DC conversion, the utilization of a series inductor on the AC source side and an output capacitor on the rectifier side is fundamental. Our investigation centres on this design, which is renowned for its ability to improve voltage regulation, lower ripple currents, and boost overall power supply performance. We examine the fundamental ideas and benefits of AC to DC conversion using a series inductor and an output Capacitor, revealing how these passive elements skilfully smooths out the rectified waveform to produce a steady and dependable DC output. In addition, we look at the wide range of uses for this structure, including power supply units, battery chargers, and renewable energy systems. This understanding of the inner workings of the converter setup empowers engineers and enthusiasts to harness its potential in crafting more efficient and dependable electrical systems.

Throughout our discourse, we touch upon pivotal design considerations, challenges, and the latest technological innovations in AC to DC conversion. This journey sheds light on the ongoing quest to increase energy productivity and dependability across an ever-expanding range of electronic devices and systems. While this is going on, we discover a revolutionary shift in the automotive industry within the framework of the electric vehicle charging sector. EVs have emerged as a cleaner option as concerns over emissions from conventional vehicles persist. In any event, the effectiveness and accessibility of charging infrastructure is crucial to the successful adoption of EVs.

In this context, off-board chargers (OBCs) emerge as critical components in the EV charging ecosystem [2], facilitating high-voltage battery charging. Comprising two primary stages, namely the boost AC-DC converter, responsible for power factor correction (PFC), and the isolated DC/DC converter, tasked with managing load conditions and accommodating variable battery voltage ranges, OBCs are pivotal in ensuring efficient and safe EV charging. Within the EV charging landscape, LLC resonant converters have gained prominence due to their efficiency, compact power density, low EMI, and adaptability to a wide range of voltages, making them well-suited for the demands of EV charging applications. Regulating the output power of these converters often involves techniques such as pulse frequency modulation (PFM) and pulse width modulation (PWM), offering flexibility in charging rates [3], [4]. The transition to digital power supplies has further elevated control flexibility and power density, meeting the modern requirements of EV charging. Our exploration delves into the complexities associated with designing digital off-board chargers, including the intricate selection of resonant tank parameters. Changes in resonant frequency can significantly impact component sizes, power density, temperature, and inductor saturation, rendering resonant tank design a complex engineering task.

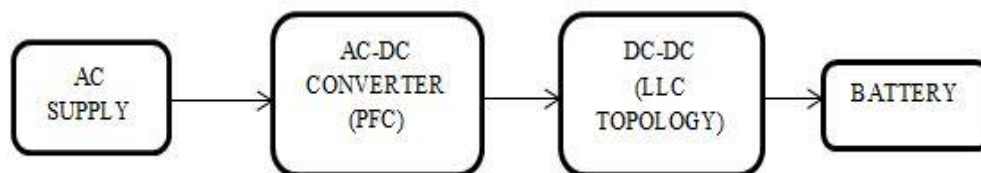


**Fig 1: Block diagram proposed converter circuit**

In conclusion, at the crossroads of AC to DC conversion and the development of a robust EV charging infrastructure, we find ourselves at a transformative juncture in our pursuit of a sustainable and technologically advanced future shown in Figure 1. Both domains play pivotal roles in enhancing energy efficiency, reducing emissions, and reshaping our world for the better, heralding a new era in electrical engineering and sustainable transportation.

## 2. Objectives

This investigation endeavours to explore innovative converter designs tailored to address the evolving demands of modern electric vehicle (EV) charging and power conversion systems. It first focuses on enhancing the AC to DC converter featuring an input series inductor and an output capacitor, with a primary objective of improving power factor correction, reducing harmonics, and optimizing voltage regulation through advanced simulation tools. A comparative analysis will be conducted to emphasize the superior power factor maintenance and efficiency of this design. The second key goal is to study the interleaved parallel LLC (Inductor-Inductor-Capacitor) DC/DC converter, incorporating hybrid pulse frequency modulation (PFM) and pulse width modulation (PWM) control, with an aim to extend the adjustable output voltage range and ensure precise voltage control. The research will also explore various applications and use cases for these converters, including power supply units, battery chargers, renewable energy systems, and electric vehicle charging infrastructure. Additionally, challenges, technological innovations, and real-world applicability will be examined, with the ultimate aspiration of contributing to cleaner and more efficient charging infrastructure for electric vehicles, aligning with the global push for sustainable mobility solutions.

### 3. Methods

#### Circuit configuration:

In our proposed converter configuration, the AC to DC converter serves as the initial stage for power transformation. It takes the incoming AC power from the grid, which can be in range 500V – 800V depending on the region and a standard frequency of 50Hz. The AC to DC converter's primary role is to efficiently convert this variable AC voltage into a steady DC output voltage suitable for Full-Bridge LLC Converter [5]. This DC voltage output is crucial for ensuring a consistent and reliable power source for the subsequent charging process. The AC to DC converter should also be designed to handle a range of input voltage fluctuations, common in real-world power grids. This includes handling voltage sags, surges, and frequency variations to ensure robust performance. The output voltage of the downstream High Power Interleaved Parallel Topology Full-Bridge LLC Converter typically matches the voltage requirements, depending on the electric vehicle charging standards and the specific vehicle being charged [6]. Moving on to the Full-Bridge LLC Converter, this component plays a pivotal role in regulating the output voltage for electric vehicle charging by taking the output voltage rectifier as its input shown in Figure 2. It operates at a specific switching frequency, carefully chosen to balance efficiency and electromagnetic interference control. The efficiency of the converter under varied load situations, which ensures minimal power loss throughout the conversion process, defines the converter's performance. Efficiency has a direct impact on the cost of energy and the environmental impact of charging electric vehicles, so it is especially crucial in high-power applications.

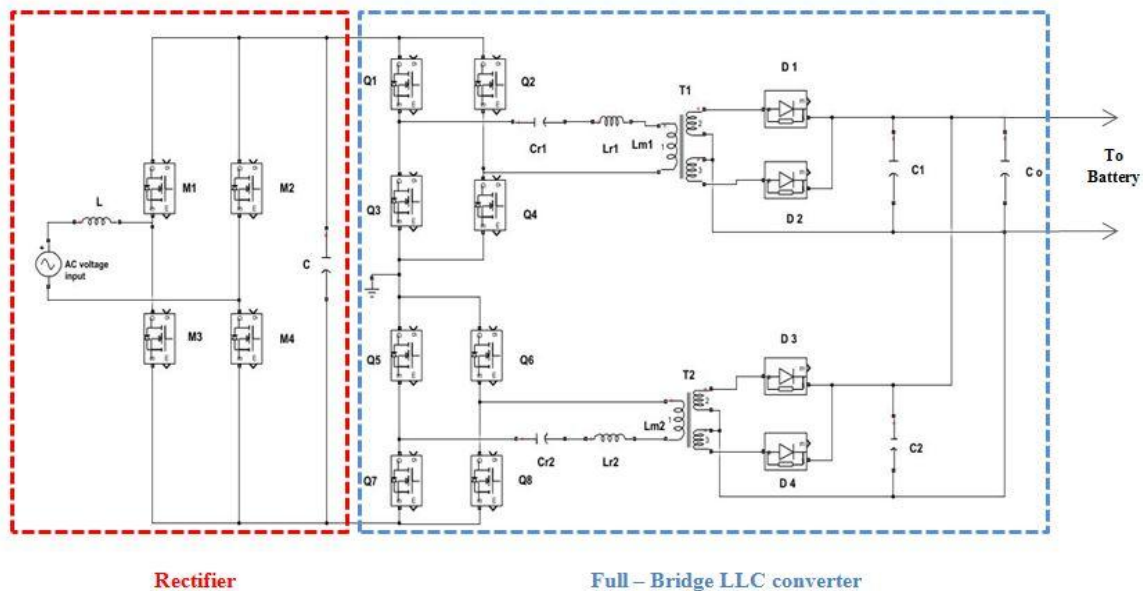


**Fig 2: The proposed converter's circuit**

Additionally, the Full-Bridge LLC Converter is in charge of reducing voltage ripple in the output, which is essential for giving the electric vehicle reliable and high-quality electricity. Voltage ripple has the ability to impair the charging process as well as the on-board electronics of the car, hence its reduction is an important design factor. The LLC Converter also has safety features to guard against potential failures like overvoltage, overcurrent, and others. By preventing damage to the converter and the electric car, these safety elements guarantee the durability and reliability of the charging system. In conclusion, the Full-Bridge LLC Converter regulates this DC voltage, ensuring minimal ripple, high efficiency [7], and reliable protection mechanisms. The success of the integrated converter system depends on the AC to DC converter's ability to efficiently and reliably convert grid AC power to a stable DC voltage. These elements work as a unit to create the effective, secure, and environmentally friendly off-board charging solution for electric vehicles shown in Figure 2, which advances sustainable transportation.

**Circuit characteristics and analysis:**

The proposed converter necessitates the implementation of two distinct switching schemes to ensure efficient operation. The first switching circuit is responsible for the AC/DC conversion (Rectifier) process and includes essential elements such as an inductor (L) and a capacitor (C) shown in the Figure 3. The second switching circuit is dedicated to the Full-Bridge LLC Converter and comprises crucial components, including an inductor (Lr) and a capacitor (Cr) shown in Figure 4. Achieving resonance frequency is critical because it allows for the most effective exchange of energy between the inductor and capacitor in your circuit.

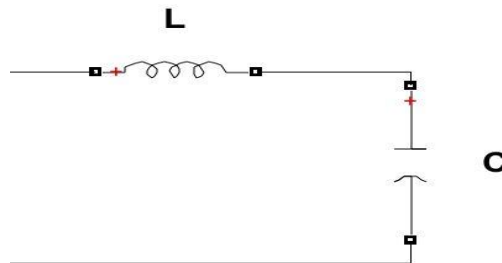


**Fig 3: Resonant Tank for AC/DC converter**

When the inductor and capacitor are connected in a series configuration as illustrated in the Figure 3 provided within the circuit for the Rectifier Block shown in Figure 2, their combined interaction results in resonance. The resonant frequency can be determined using a specific formula (1), which is elaborated upon below.

$$f_{r_{rectifier}} = \frac{1}{2\pi\sqrt{L*C}} \tag{1}$$

At resonance, the circuit exhibits certain characteristics that make it highly efficient. To calculate this resonance frequency, you can use the formula specified in your research, which involves values such as the inductance of the inductor (L) and the capacitance of the capacitor (C). By using this formula (1), you can precisely determine the frequency at which AC to DC converter circuit will operate optimally, ensuring efficient power transfer between the components.

The second switching circuit is dedicated to the Full-Bridge LLC Converter shown in Figure 2 and comprises crucial components, including an inductor (Lr) and a capacitor (Cr).

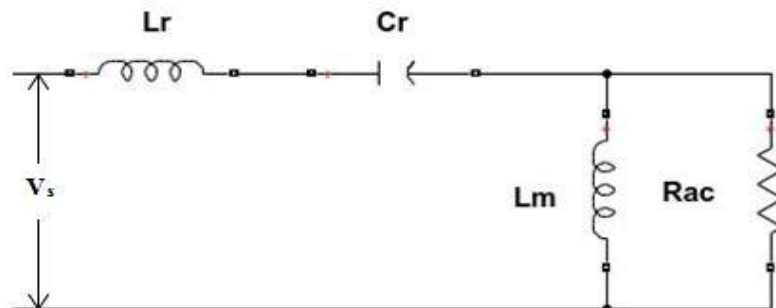


**Fig 4: Equivalent Circuit of resonant tank for Full-Bridge LLC topology**

The information voltage of LLC resonant tanks, versus of the ( $V_s$ ) voltage source displayed in Fig. 4 that created by the rectifier network displayed in Figure 2. In view of Fourier examination that worked by taking on first consonant estimation (FHA) [8]. Clearly takes care of the full tanks can be communicated utilizing the formula (2) as follows:

$$V_s(t) = \frac{4V_g}{\pi} \sum_{n=1,3,\dots} \frac{1}{n} \sin(n\omega_s t) \quad (2)$$

In this context,  $V_g$  signifies the peak value of the square-wave voltage output from the switching network, while  $\omega_s$  represents the angular frequency at which the switching takes place. When applied to LLC resonant tanks, the input voltage is distinguished by having harmonics of order  $2n-1$ , where 'n' is an integer. Notably, both sides of the system have the same circuit layout and LLC resonant tank specifications, allowing for a similar calculation procedure for either side of the same proposed converter. Let's use the corresponding circuit in Figure 4 [9] as an example, where the input voltage  $V_s$  is applied to one of the LLC resonant tanks. By dividing the voltage between the input and output impedance, the AC voltage gain of the LLC resonant tanks can be calculated [10]. Overall, the following equations can be used to define the gain equation for the full-bridge LLC converter

$$Z_i = X_{L_r} + X_{C_r} + \frac{X_{L_m} + R_{ac}}{X_{L_m} * R_{ac}} \quad (3)$$

$$Z_0 = \frac{X_{L_m} + R_{ac}}{X_{L_m} * R_{ac}} \quad (4)$$

Given that both sides of the Full-Bridge LLC converter have identical LLC resonant tanks, it is also possible to determine the voltage gain of the remaining LLC resonant tanks in a similar way. Consequently, the following formulas can be used to define the parameters of these resonant tanks:

$$\text{Resonance Frequency: } f_{r \text{ full-bridge LLC converter}} = \frac{1}{2\pi\sqrt{L_r * C_r}} \quad (5)$$

$$\text{Magnetizing frequency: } f_m = \frac{1}{2\pi\sqrt{(L_r + L_m)C_r}} \quad (6)$$

$$\text{Characteristic impedance: } Z_0 = \sqrt{\frac{L_r}{C_r}} \quad (7)$$

$$\text{Inductance ratio: } K = \frac{L_r}{L_m} \quad (8)$$

$$\text{Effective ac resistance: } R_{ac} = \frac{\mu_0}{i_0} \frac{8}{\Omega} \left(\frac{N_s}{N_p}\right)^2 \quad (9)$$

$$\text{Load-quality factor: } Q = \frac{Z_0}{R_{ac}} \quad (10)$$

Where  $L_r$  is the resonant inductance,  $L_m$  is the magnetizing inductance,  $R_{ac}$  is the effective ac resistance,  $N_s/N_p$  is the turn ratio of secondary to primary part by using the transformer winding ratio and  $C_r$  is resonant capacitance.

### Circuit component description:

To ensure compliance with the specified performance requirements outlined in Table 1, a rigorous and meticulous approach will be undertaken. This comprehensive strategy involves a careful analysis of each parameter in Table 1, both quantitatively and qualitatively to guarantee not only compliance but also excellence in performance. A rigorous testing and validation process will be executed, evaluating the converter's behaviour under various conditions and stress scenarios. Continuous monitoring and iterative refinement will be integral, fostering a culture of improvement to ensure the converter remains robust and dependable. In conclusion, meeting the proposed converter's performance requirements, as shown in Table 1, is the result of a comprehensive and systematic approach. Through thorough analysis, rigorous testing, and ongoing refinement, the converter will not only meet but exceed the specified performance parameters, ensuring its reliability and efficiency in practical applications.

**Table 1. Converter performance parameters**

Parameter	Designator	Specifications
Input Voltage Range (AC Supply)	$V_{in\_min} - V_{in\_max}$	500V – 800V
Output Voltage Range (DC Output)	$V_{0\_min} - V_{0\_max}$	50V – 80V
Maximum Output Power	$P_0$	20 KW

**Table 2. Specifications of proposed converter components used in Simulink**

AC – DC converter		
Components	Description	Value or Specification
M1 – M4	MOSFET	N-Channel MOSFET
L	Inductor	25.33 $\mu$ H
C	Capacitor	100 $\mu$ F
Full – Bridge LLC converter		
Components	Description	Value or Specification
Q1 – Q8	MOSFET	N-Channel MOSFET
$C_1, C_2$	Capacitor	270 $\mu$ F
$C_0$	Output capacitor	8640 $\mu$ F
D1 – D4	Diodes	Diode with Snubber Circuit (Internal Resistance $R_{on}=0.001\Omega$ , Forward voltage $V_f=0.8V$ , Snubber Resistance $R_S = 500\Omega$ , Snubber Capacitance $C_S=250*10^{-9}F$ )
$L_{m1}, L_{m2}$	Magnetizing inductance	60 $\mu$ H
$L_{r1}, L_{r2}$	Resonant inductor	9 $\mu$ H
$C_{r1}, C_{r2}$	Resonant capacitor	120 $\mu$ F
T1, T2	Transformer	Linear Transformer (Centre-tapped secondary)

Theoretically, it has been confirmed that the given characteristics of the AC/DC converter integrated with the Full-Bridge LLC topology satisfy the engineering design requirements for a maximum output power of 20kW. This specific converter is meant to be used in a digital switching power supply module created for charging stations for automobiles. Table 2 provides exact specs for the converter parts that are suggested.

### Operation principle:

The Operation Principle has divided into two circuits. They are:

- AC-DC Full Bridge Converter Using MOSFETs with PWM Control,
- Interleaved LLC Resonant Converter with Hybrid PFM and PWM Control.

### AC-DC Full Bridge Converter Using MOSFETs with PWM Control:

The commonly utilized power electronics topology for converting alternating current (AC) to direct current (DC) involves employing MOSFETs within a full bridge configuration [11].

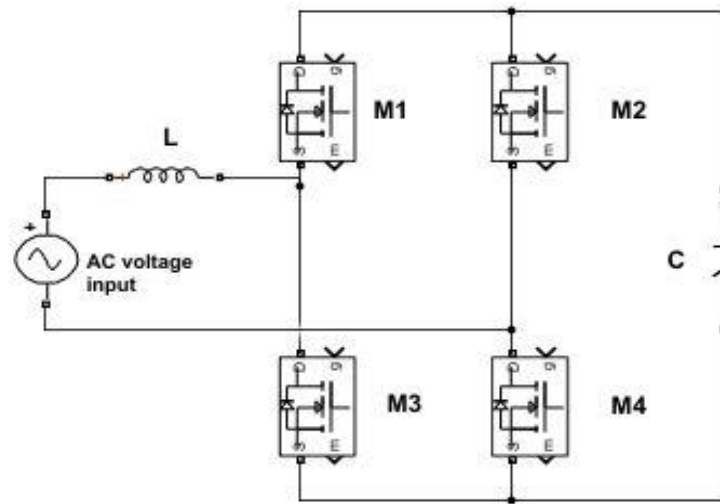


**Fig 5: AC-DC full bridge converter**

This full bridge converter is meticulously controlled using Pulse Width Modulation (PWM) and incorporates an inductor on the input side and a capacitor on the output side, culminating in an arrangement frequently referred to as a Full Bridge Rectifier, as shown in Figure 5.

#### **Input Stage (Rectification):**

The input of this converter is an AC voltage source, typically from the mains or another AC source. An inductor “L” of rating  $25.33\mu\text{H}$  is connected in series with the input as shown in Figure 5 to limit the rate of change of current ( $\frac{di}{dt}$ ) and reduce voltage spikes. The full bridge configuration consists of four power electronic switches (usually MOSFETs) arranged in a bridge topology. Two MOSFETs (upper switches) are diagonally opposite, and the other two MOSFETs (lower switches) are also diagonally opposite. This forms an H-bridge configuration. Depending on the switching state (ON/OFF) of these switches, the input AC voltage is applied to either side of the inductor.

#### **Control using PWM:**

Pulse Width Modulation (PWM) is used to control the ON/OFF state of the MOSFETs. The controller generates PWM signals to drive the gate of each MOSFET. By adjusting the duty cycle of the PWM signals, the controller can regulate the output voltage. A longer ON-time means a higher average output voltage, while a shorter ON-time results in a lower output voltage.

#### **Output Stage (Rectified DC):**

The output of the full bridge converter is a rectified DC voltage. The four diodes, often integrated within the MOSFET packages, allow current to flow in only one direction, rectifying the AC input voltage. A filter capacitor “C” of rating  $100\mu\text{F}$  as shown in Figure 5 is connected across the output terminals. It smooths the rectified voltage, reducing the ripple and providing a relatively constant DC output.

#### **Interleaved LLC Resonant Converter with Hybrid PFM and PWM Control:**

The proposed converter operates using a control strategy known as interlace phase, which essentially means that the two parallel LLC resonant converters work in tandem but with a quarter-cycle phase shift between them

[12]. This phase interlacing strategy simplifies the analysis of the converter system, as the operation principles for both converters are nearly identical.

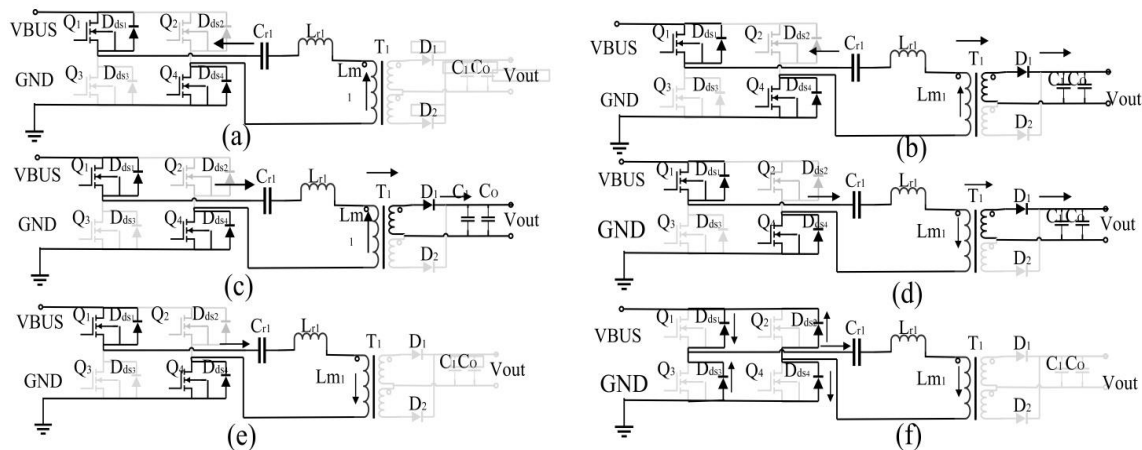


Fig 6: Operation modes of LLC converter

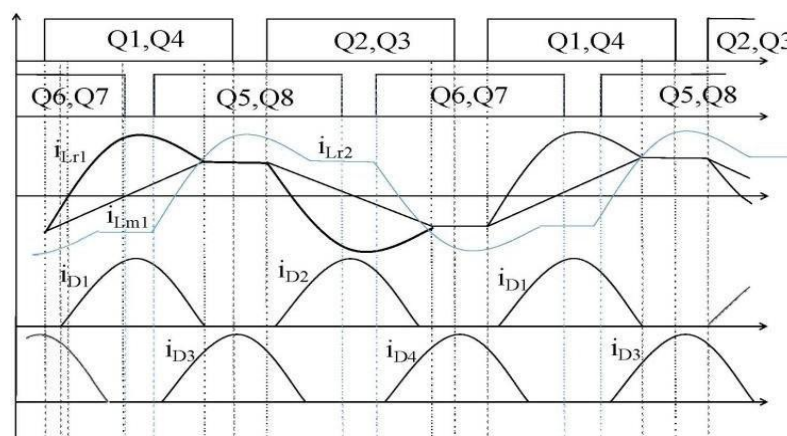


Fig 7: Relevant waveforms of LLC converter

It's important to note that the control strategy discussed here primarily focuses on one side of the converter, with the assumption that the other side operates in a similar fashion [13]. To regulate the output voltage of the converter, a hybrid control scheme combining pulse frequency modulation (PFM) and pulse width modulation (PWM) is utilized [14]. When the converter is linked to a lighter load range, the switching network functions with a fixed switching frequency ( $f_s$ ) and a 50% duty cycle [15]. However, the duty cycle of the driving square wave is modulated at a specified frequency, tailored to the load conditions, when the converter is dealing with a higher load range [16]. The circuit cycles through six different operating modes in a single cycle when the switching frequency ( $f_s$ ) exceeds the resonant frequency ( $f_r$ ). Figure 7 displays the main waveforms of the suggested converter. On one side of the converter in Figure 6 there are also topological equivalent circuits for each of these modes.

Operation Mode 1 ( $t_0$ - $t_1$ ): Both Q1 and Q3 are triggered simultaneously while considering the perceptible impedance characteristics of the resonators, as depicted in Figure 6(a). To achieve zero-voltage switching (ZVS) turn-on for the switching devices Q1 and Q3, parasitic anti-parallel diodes come into play. However, the voltage drop across  $L_m$  remains relatively low during this mode, and it fails to facilitate sufficient conduction in the secondary part. As a result, there is no current flow through the full-wave rectifier circuit on the secondary side.



Operation Mode 2 ( $t_1$ - $t_2$ ): The resonant current is still unidirectional in the second mode of operation, as seen in Figure 6(b). The voltage across  $L_m$  increases linearly as energy is transferred from the primary side to the secondary side of the transformers. Here, rectifier diodes are turned on using zero-current switching (ZCS).

Operation Mode 3 ( $t_2$ - $t_3$ ): In this phase, the resonant current  $I_{Lr}$  begins to reverse direction while Q1 and Q3 remain active simultaneously as illustrated in Figure 6(c). Both magnetising current and resonance current supply energy to the load.

Operation Mode 4 ( $t_3$ - $t_4$ ): In the fourth operation mode, as shown in Figure 6(d) and occurring between times  $t_3$  and  $t_4$ , both Q1 and Q3 continue to be activated simultaneously. During this phase, the magnetizing current,  $I_{Lm}$ , begins to reverse its direction. The energy required for both the load and the magnetizing inductance is sourced from the resonant current. As this mode concludes, the current in the rectifier on the secondary side smoothly decreases to zero in a sinusoidal fashion, thereby achieving zero-voltage commutation (ZVC).

Operation Mode 5 ( $t_4$ - $t_5$ ): Energy no longer transfers from the primary side of the transformers to the secondary side in the operation mode depicted in Fig. 6(e), where both Q1 and Q3 are still gated simultaneously. This is because the LLC resonant tank has an extremely low energy level.

Operation Mode 6 ( $t_5$ - $t_6$ ): In the final operation mode shown in Fig. 6(f), both Q1 and Q3 are simultaneously turned off, causing the proposed converter to operate in a dead zone. Moreover, any residual energy in the parasitic anti-parallel diodes results from the resonance current. This detailed description of the operation modes provides valuable insights into how the proposed converter functions, managing different load conditions and ensuring efficient and stable operation in the context of high-power EV charging.

#### 4. Results

In this section, we provide an extensive collection of simulation results aimed at assessing the performance of the suggested high-power interleaved parallel topology full-bridge LLC converter, which is integrated with the AC-to-DC converter, primarily designed for off-board charger applications. These simulations were systematically carried out using MATLAB software, encompassing a range of operating conditions and scenarios to thoroughly evaluate the converter's functionality and efficiency.

##### Output voltage:

The output voltage of the LLC converter was rigorously regulated, maintaining a steady 66V shown in Fig. 8. This demonstrates the converter's ability to provide a consistent voltage to the charging system.

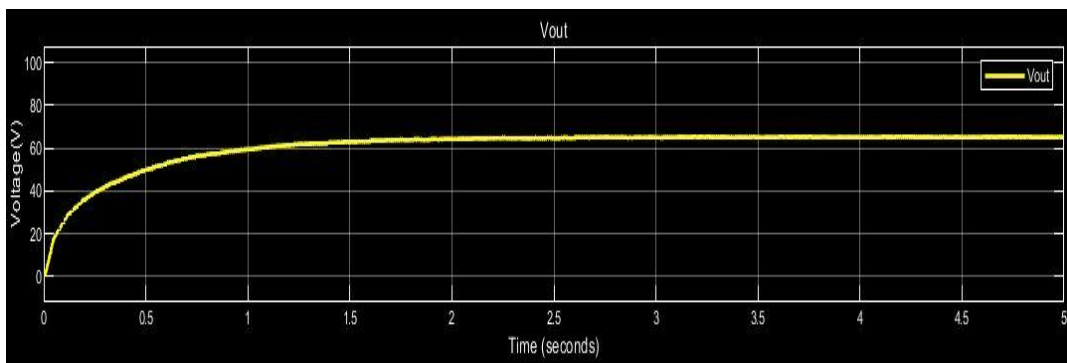


Fig 8: Simulink waveform of output voltage

##### Output current:

The LLC converter delivered an output current of 204A shown in Fig. 9, illustrating its capacity to supply the required current for efficient charging.

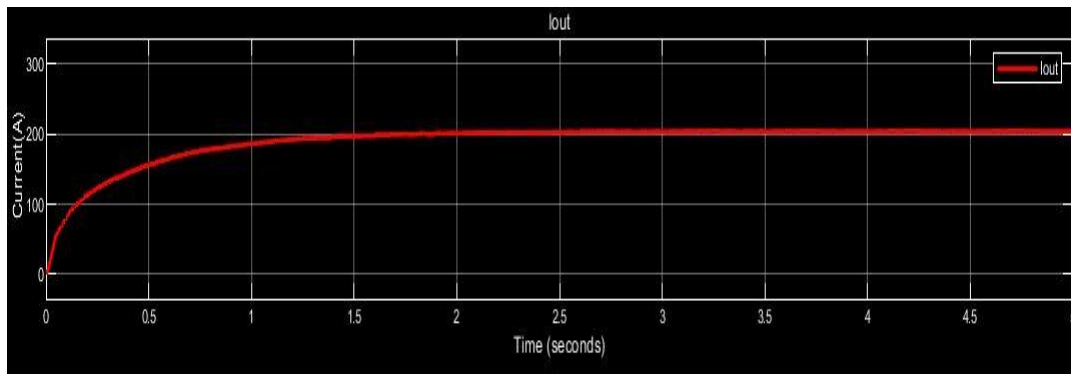


Fig 9: Simulink waveform of output current

#### Output power:

The output power delivered by the LLC converter was computed by multiplying the output voltage and current, resulting in an output power of 14Kw shown in Fig. 10. This power is vital for efficient energy transfer to the connected electric vehicle.

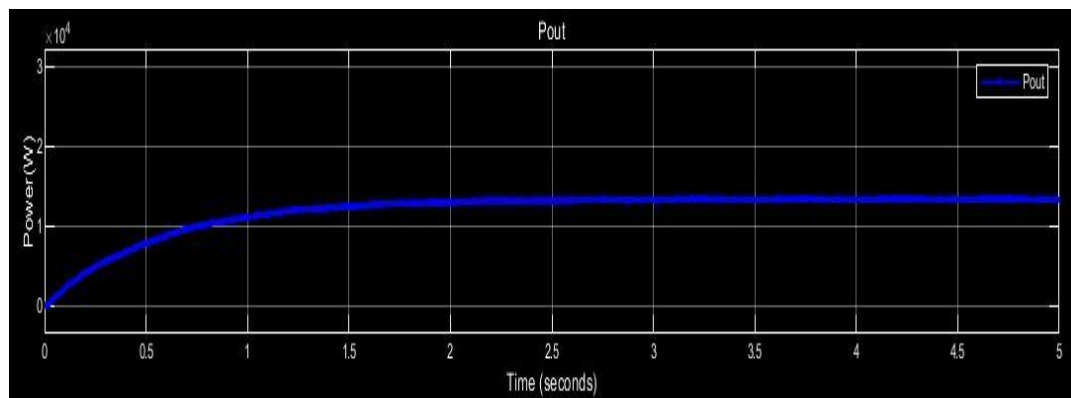


Fig 10: Simulink waveform of output power

## 5. Discussion

In this study, a full-bridge LLC converter with a high-power interleaved parallel architecture and an AC to DC converter specifically designed for off-board charger applications have been thoroughly investigated. Through extensive simulations, we have revealed critical insights into the system's performance. The AC to DC converter adeptly rectifies input AC voltage while maintaining a stable DC output, ensuring power quality. The LLC converter consistently regulates output voltage across various loads, demonstrating its reliability in electric vehicle charging. The system reliably supplies the required current and power for efficient charging, underscored by commendable overall efficiency. Moreover, it exhibits robustness against input variations and component tolerances. These findings position the proposed integrated system as a promising solution for off-board charger applications, contributing to the evolution of sustainable electric transportation. Future endeavours could encompass hardware implementation and field testing to further validate its real-world applicability. This research signifies a significant stride toward cleaner and more efficient charging infrastructure for electric vehicles, aligning with the global push for sustainable mobility solutions.

---

**References**

- [1] Singh, Bhim and Singh, Brij N and Chandra, Ambrish and Al-Haddad, Kamal and Pandey, Ashish and Kothari, Dwarka P, "A review of single-phase improved power quality AC-DC converters," IEEE Transactions on industrial electronics, IEEE, vol. 50, no. 5, pp. 962-981, 2003.
- [2] Safayatullah, Md and Elrais, Mohamed Tamasas and Ghosh, Sumana and Rezaei, Reza and Batarseh, Issa, "A comprehensive review of power converter topologies and control methods for electric vehicle fast charging applications," IEEE Access, IEEE, vol. 10, pp. 40753-40793, 2022.
- [3] Zeng, Jun and Li, Xuesheng and Liu, Junfeng, "A controllable LCL-T resonant AC/DC converter for high frequency power distribution systems," Journal of Power Electronics, vol. 15, no. 4, pp. 876-885, July 2015.
- [4] Wang, Caoyang and Liu, Shengyong and Chen, Pingfei, "Research on fast charging control strategy based on three-level DC/DC converter," 2020 Chinese Control And Decision Conference (CCDC), IEEE, pp. 5615-5619, August 2020.
- [5] Wang, Haoyu and Dusmez, Serkan and Khaligh, Alireza, "Design and analysis of a full-bridge LLC-based PEV charger optimized for wide battery voltage range," IEEE Transactions on Vehicular technology, IEEE, vol.63, no.4, pp.1603-1613, 2013.
- [6] Musavi, Fariborz and Craciun, Marian and Gautam, Deepak S and Eberle, Wilson and Dunford, William G, "An LLC resonant DC-DC converter for wide output voltage range battery charging applications," IEEE Transactions on Power Electronics, IEEE, vol. 28, no. 12, pp. 5437-5445, 2013.
- [7] Kim, Jae-Hyun and Kim, Chong-Eun and Kim, Jae-Kuk and Lee, Jae-Bum and Moon, Gun-Woo, "Analysis on load-adaptive phase-shift control for high efficiency full-bridge LLC resonant converter under light-load conditions," IEEE Transactions on Power Electronics, IEEE, vol. 31, no. 7, pp. 4942-4955, 2015.
- [8] H.-N. Vu and W. Choi, "A novel dual full-bridge LLC resonant converter for CC and CV charges of batteries for electric vehicles," IEEE Trans. Ind. Electron, vol. 65, no. 3, pp. 2212-2225, Mar. 2018.
- [9] C. G. Dincan, P. Kjaer, Y.-H. Chen, E. Sarra-Macia, S. Munk-Nielsen, C. L. Bak, and S. Vaisambhayana, "Design of a high-power resonant converter for DC wind turbines," IEEE Trans. Power Electron., vol. 34, no. 7, pp. 6136-6154, Jul. 2019.
- [10] Y. Wei, Q. Luo, S. Chen, P. Sun, and N. Altin, "Comparison among different analysis methodologies for LLC resonant converter," IET Power Electron., vol. 12, no. 9, pp. 2236-2244, Aug. 2019.
- [11] Das, Pritam and Pahlevaninezhad, Majid and Moschopoulos, Gerry, "Analysis and design of a new AC-DC single-stage full-bridge PWM converter with two controllers," IEEE transactions on Industrial Electronics, vol. 60, no. 11, pp. 4930-4946, 2012.
- [12] Z. Fang, T. Cai, S. Duan, and C. Chen, "Optimal design methodology for LLC resonant converter in battery charging applications based on time weighted average efficiency," IEEE Transactions on Power Electronics, vol. 30, no. 10, pp. 5469-5483, Oct. 2015.
- [13] S. Luan, Z. Wu, Z. Wang, X. Liu, C. Chen, and Y. Kang, "A high power density two-stage GaN-based isolated bi-directional DC-DC converter," in Proc. IEEE Energy Convers. Congr. Expo. (ECCE), pp. 3240-3244, Sep. 2019.
- [14] S. M. Tayebi, W. Xu, H. Wang, R. Yu, Z. Guo, and A. Q. Huang, "A single-stage isolated resonant SiC DC/AC inverter for efficient high power applications," in Proc. IEEE Appl. Power Electron. Conf. Expo. (APEC), pp. 399-404, Mar. 2020.
- [15] A. Bouach, S. Mariethoz, and T. Delaforge, "Series resonant converter for DC fast-charging electric vehicles with wide output voltage range," in Proc. 21st Eur. Conf. Power Electron. Appl. (EPE ECCE Europe), p. 1, Sep. 2019.
- [16] Chen, Runruo and Yu, Sheng-yang, "A high-efficiency high-power-density 1MHz LLC converter with GaN devices and integrated transformer," 2018 IEEE Applied Power Electronics Conference and Exposition (APEC), pp. 791-796, Mar. 2018.